Check for updates

Phonons of Phase-Change Materials

Jean-Pierre Gaspard

Phase-change materials (PCMs) undergo a reversible transition from a semi-conducting to a metallic state, nicely termed "incipient metal." This transition is driven by a Peierls distortion. A model of covalent bonding is developed in a tight-binding scheme that accounts for the drastic evolution of some properties of PCMs, among which the Grüneisen parameter. The original vibrational properties of PCM and related Peierls distorted materials are analyzed. A three-body covalent interaction describes the PCM properties. It explains the simultaneous softening of the optical phonons and the hardening of the acoustic phonons upon crystallization of the PCMs.

1. Introduction

Phase-change materials (PCMs) are materials characterized by a drastic change of their electronic and optical properties when they switch from the amorphous to the crystalline phase.[1,2] This transition is fast and qualifies them for nonvolatile memory applications. Most PCMs are Te compounds. They have a portfolio of remarkable properties: a moderate electrical conductivity, an anomalous coordination number, a high Grüneisen parameter, a high dielectric constant ε_∞, and a high Born charge Z*. These outstanding properties originate in the chemical bond. The bonding in PCMs has long been debated[3] and various models have been suggested, among which resonant bonding,[4] meta-valent bonding,[5] and multicenter hyperbonding.[6] The specific properties of PCMs are related to their electronic properties: they are at the borderline between a semiconductor and a metal, hence the evocative name "incipient metal."[5] The transition from a metallic phase to a distorted semiconducting phase is driven by the Peierls distortion,[7–11] a symmetry breaking mechanism. Large anharmonicities play a role in the electrical, optical, and thermoelectric properties of PCM.[12,13] Upon crystallization to a less distorted metallic structure, the vibrational acoustic modes harden while the optical modes soften,[14] an unusual behavior.

The aim of this article is to show that a minimal model of covalent bonding explains the remarkable properties of PCMs with a particular emphasis on the vibrational properties.

J.-P. Gaspard
University of Liège
SPIN-CESAM, B5, B-4000 Sart-Tilman, Belgium
E-mail: jp.gaspard@uliege.be

J.-P. Gaspard
Laue-Langevin Institute, Theory Group
F-38042 Grenoble Cedex 9, France

The ORCID identification number(s) for the author(s) of this article can be found under https://doi.org/10.1002/pssr.202200111.

The motivations of this article are multiple: 1) analysis of the bonding and vibrational properties of covalent materials in the vicinity of the vanishing harmonicity conditions;[13] 2) study of the origin of the anomalous behavior of the Grüneisen parameter; 3) relation to the negative temperature expansion[15,16] in parent compounds; and 4) universality of the behavior of covalent Peierls distorted structures.

2. Model

The structure of covalent compounds made of atoms of the right-hand part of the periodic table is dominated by the σ bonding of p orbitals in a possibly distorted octahedral structure with partial filling of the p band. The cohesive energy originates from the broadening of the p band whose effective width is given by the square root of the second moment μ_2 of the electronic density of states $n_p(E)$.[17] μ_2 is proportional to the number Z of nearest neighbors; thus, the cohesive energy is proportional to the square root of the coordination number. As a consequence, the contributions of the individual interatomic bonds are not additive; this is crucial for the understanding of the properties of covalent structures, in particular the PCMs. We take into account the $pp\sigma$ coupling, neglecting the (weaker) $pp\pi$ coupling. We assume that the lower energy s-levels are filled and do not play an appreciable role in cohesion (no sp hybridization). In this case, because of the orthogonality of the p orbitals, the 3D electronic spectrum of an octahedral structure can be decomposed into three 1D independent spectra, an appreciable simplification.

In addition, the partial filling of the p band induces a Peierls distortion[7,18] if the repulsion is not too strong[19] (**Figure 1**). Short and long bond alternates and consequently an electronic gap opens. The Peierls distortion of an octahedral structure leads to a coordination number $Z = 6 - N_p$[8] where N_p is the number of p electrons per atom, more usually written $Z = 8 - N_{sp}$, the celebrated octet rule.

The octet rule is a simplification/idealization in which two neighboring atoms are considered bonded or not depending on their distance. In simple monoatomic crystalline structures, the situation is relatively clear: e.g., the coordination number is 3 for antimony and 2 for tellurium. More precisely, one should better write, respectively, 3(+3) and 2(+4) as discussed in ref. [8]. Only when the interatomic separations are grouped into a bunch of short distances distinct from the longer distances, the counting of bonds is obvious. In amorphous or liquid structures, the distribution of distances is continuous (e.g., ref. [16]) and the definition of a bond is somewhat arbitrary. In crystalline structures under pressure, the bond lengths evolve continuously and the fulfilling or not of the octet rule is subject to some arbitrariness.

ADVANCED SCIENCE NEWS
www.advancedsciencenews.com

pssrrl
physica status solidi
www.pss-rapid.com

Figure 1. A dimerized linear chain. Reproduced with permission.[13] Copyright 2021, Wiley-VCH.

For a half-filled p band, the equilibrium structure is a Peierls distorted dimerized chain with two alternating distances D_S and D_L (Figure 1).

This is the case we will concentrate on for simplicity; the extension to other band fillings and distortions is obvious.[8]

The cohesive energy is approximated, in a simple tight binding scheme, by the sum of an attractive resonance σ interaction of the p orbitals and an effective pairwise repulsion energy.

The resonance integral of the covalent σ bond varies with the distance r as $\sigma(r) = \beta_0/r^q$. The repulsion is approximated by $V_R(r) = V_0/r^p$; the parameter p does depend on the nature of the atoms. The energy is given, by atom, by

$$E = -\frac{\beta_0}{\sqrt{2}}\sqrt{\frac{1}{D_S^{2q}} + \frac{1}{D_L^{2q}}} + \frac{1}{2}V_0\left(\frac{1}{D_S^p} + \frac{1}{D_L^p}\right) \qquad (1)$$

where D_S and D_L are the short and long interatomic separations. The square root comes from the second moment approximation. One is above a simple pair potential: the interaction involves three successive atoms ($i-1$, i, and $i+1$). These three-body interactions are a key point for the Peierls symmetry breaking mechanism.

For a quantitative analysis, the model presented here requires four parameters: p, q, β_0, and V_0. Taking $q = 2$ according to Harrison,[20] the remaining three parameters p, β_0, and V_0 could be obtained by fitting to the cohesive energy, interatomic distance, and compressibility. Instead, to analyze the general behaviors of the model, in this work I have chosen $\beta_0 = 1$. To impose that the equilibrium distance is equal to 1 for an undistorted chain, I have taken $V_0 = p/q$. With these additional conditions, a single parameter is remaining: p (or p/q). This parameter fixes the amplitude of the Peierls distortion as compiled in **Table 1**. Consequently, all plots will be presented in arbitrary units in order to concentrate on the mechanisms and trends that are produced by this model.

If the two interatomic separations D_S and D_L are equal, Equation (1) reduces to the classical Mie potential,[21] which is a pair potential.

In this minimal model of the covalent bond, the system is assumed to be composed of identical averaged atoms. The modest charge transfer in PCM is disregarded. We stress that the model (1) is local and as such can be applied to crystalline, amorphous, or liquid structures.

The tight-binding model (1) connects three sites. It has some analogy within the model of multicenter hyperbonding[6] but

with a totally different approach. Despite the fact that the energy depends only on the distances, the energy is not pair additive because of the square root in (1). This plays a central role in the structural and the vibrational properties as we will see.

The second term of (1) is the effective repulsion characterized by an effective exponent p.[22,23] The heavier the element, the larger is the number of closed shells, the harder is the repulsive term, and the larger is the p-value. The parameters p and q determine whether the structure is distorted or not.[8] If $p < 2q$ (soft repulsion), the structure is distorted. If $p > 2q$, the strong repulsion prevents the structure from being distorted (Table 1) and (Table 2).

The aim of this article is to analyze what kind of physical properties of the Peierls distorted structures (and PCM) a simple (minimal) 1D covalent model can account for. Of course, the model shows some limitations. The distortion in the distances implies a (small) departure of the bond angles with respect to 90° in a Euclidean space. As a consequence, the factorization of the 3D equations into $3 \times 1D$ equations is not strictly true: a correction to the second order in the angle deviation from 90° is required. By nature, the 1D model involves only the longitudinal phonons. The lone pairs are formally absent from this description. The demonstration of the octet rule[8] makes no reference to the lone pairs. Of course on a more fine scale, the lone pair should be taken into account, but the issue is still subject to discussion. For example, while in the orthorhombic GeS the lone pairs are clearly visible; in GeTe their role is questionable.[9] It is generally admitted that the opening of a gap at the Fermi energy produces an energy gain and stabilizes the distorted structure provided that the effective repulsive term does not hinder the deformation. However, this universal behavior is questioned and the role of electrostatic interactions is highlighted in some systems.[10,11] The two structures, crystalline and amorphous, have different densities. The Peierls distortion is highly sensitive to the density with important consequences on the electronic and vibrational properties. We use the pressure as a tuning parameter that drives the volume or the density (**Table 2**).

Figure 2 shows typical energy landscapes. Figure 2a corresponds to the situation where $p > 2q$; the minimum is on the ascending diagonal ($D_S = D_L$); the stable structure is a linear chain of equally spaced atoms. The repulsive potential prevents dimerization.

Figure 2c $p < 2q$, i.e., a soft repulsion, a spontaneous symmetry breaking appears; it corresponds to the Peierls distorted case with two different distances $D_S < D_L$ (Strictly, at equilibrium, the long bonds are infinitely long: a well-known artifact of the tight-binding model. However, the à la Landau development gives also a finite D_L. The stable configuration is shown by the red dot. In the three cases, the bonding is covalent.

Table 1. The occurrence of a distortion depends on the ratio $\frac{p}{q}$.[19]

p/q	Structure	Conductivity
<2	Distorted	Semiconductor
=2	Marginal	Incipient metal
>2	undistorted	Metal

Table 2. Several examples of the tight binding parameters p and q.

Compound	q	p	p/q
GeTe	2	3.5	1.75
$Ge_2Sb_2Te_5$	2	3.6	1.8
Sb_2Te	2	3.72	1.86
PbTe	2	4.2	2.1

ADVANCED SCIENCE NEWS
www.advancedsciencenews.com

pssrrl
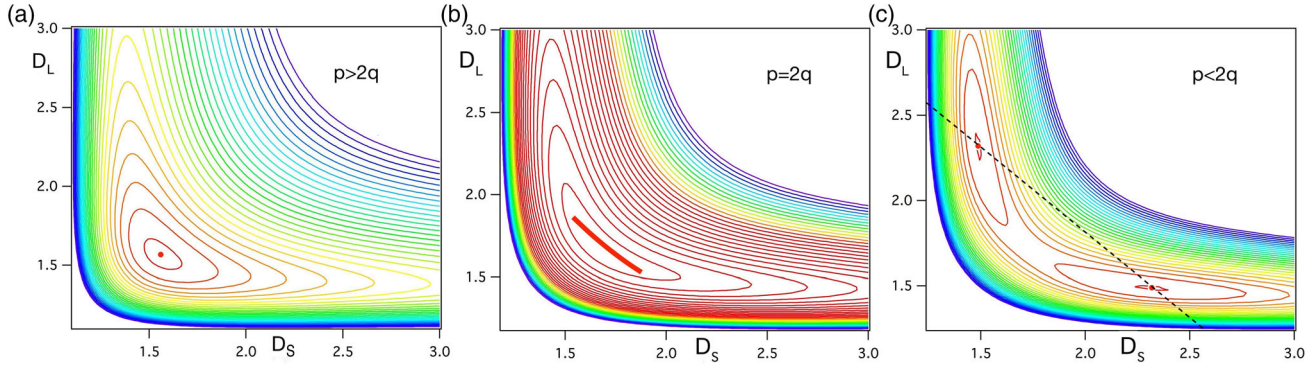physica status solidi
www.pss-rapid.com

Figure 2. Energy landscapes $E(D_S, D_L)$ as a function of the distances D_S, D_L. From left to right: a) undistorted, b) incipient metal, and c) Peierls distorted. The red dot indicates the stable configuration. In the incipient metal (b),[5] the reference point rattles along the descending red diagonal because the force constants vanish to first order. It corresponds to the red curve in Figure 3. The dotted line in panel (c) is a constant length line ($D_S + D_L$ = constant); it corresponds to the blue curve in Figure 3.

We define a dimensionless distortion parameter η.

$$\eta = \frac{D_L - D_S}{D_L + D_S} \qquad (2)$$

The energy given by Equation (1) is expanded à la Landau in a series expansion of η.

$$E(\overline{D}, \eta) = E_0(\overline{D}) + \alpha(\overline{D})\eta^2 + \gamma(\overline{D})\eta^4 = E_0(\overline{D}) + \Delta E_P \qquad (3)$$

where $\overline{D} = (D_L + D_S)/2$ is the average interatomic separation and ΔE_P is the Peierls energy, i.e., the energy gained by the distortion when $\alpha < 0$

$$\alpha(\overline{D}) = \frac{q}{2}\left[\frac{1}{\overline{D}^p}(p+1) - \frac{1}{\overline{D}^q}(2q+1)\right] \qquad (4)$$

At the equilibrium distance D_e, one has

$$\alpha(D_e) = \frac{1}{2}\frac{pV_0}{D_{eq}^p}(p - 2q) = E_{coh}(D_e)\frac{pq(p - 2q)}{2(p - q)} \qquad (5)$$

Figure 2b is the interesting marginal case where with $p = 2q$ and $\alpha = 0$, i.e., there is no restoring force in η in first order. It corresponds to the so-called "incipient metal"[5] shown in the red curve in **Figure 3**.

The interaction energy (1), expanded to second order in the displacement (harmonic expansion), differs from a harmonic potential with two force constants. The two distances D_L and D_S are correlated and the dynamical matrix has cross terms. This has important consequences on the vibrational spectrum.

The Peierls distortion is sensitive to the density (volume) of the material. The relevant difference from the amorphous (less dense) and the crystalline phases of the PCMs is their density difference by about 6% (e.g., Ge$_2$Se$_2$Te$_5$[24]). In the 1D model, we differentiate the two phases by a density variation in 1D of 2%. Even with such a low-density variation, the vibrational properties are strongly affected as one sits close to a structural transition.
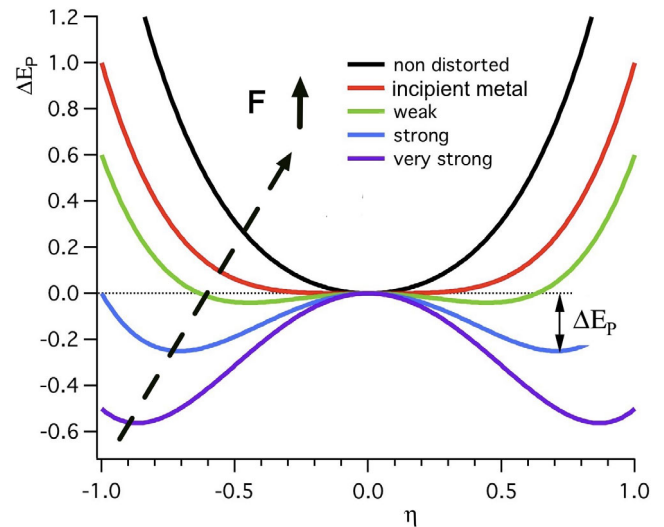

Figure 3. Evolution of the Peierls distortion energy ΔE_P as a function of η for different values of the ratio p/q. The red curve (incipient metal) corresponds to a vanishing harmonic term in η. The curves correspond to increasing pressures (force in 1D) from bottom to top.

3. Phonons

The enthalpy of a dimerized structure (Figure 1) is given by

$$H = \sum_i\left[-\frac{1}{\sqrt{2}}\sqrt{\frac{1}{D_i^{2q}} + \frac{1}{D_{i+1}^{2q}}} + \frac{q}{2p}\left(\frac{1}{D_i^p} + \frac{1}{D_{i+1}^p}\right) + PD_i\right] \qquad (6)$$

as a function of the distances D_i. The atomic positions are R_i with displacements u_i, the atomic separations are $D_i = R_{i+1} - R_i$, and their fluctuations are $\delta_i = u_{i+1} - u_i$.

An extra pressure term PD_i is added to the energy for several reasons: 1) in a simple tight binding model, the distortion is infinite ($D_L = \infty$) when it occurs in the absence of an external pressure; 2) the additional pressure simulates the neglected cohesive contributions (e.g., van der Waals interactions); 3) pressure

allows changing the volume. In 1D, the "pressure" P has the dimension of a force MLT^{-2} ($M =$ mass, $L =$ length, $T =$ time).

Of course in 1D, the notion of amorphous is difficult to define. We distinguish the amorphous and the crystalline structures by their sole density and the density is controlled by pressure.

The Taylor expansion of the energy is given by, to second order in δ_i's, at the equilibrium

$$E = E_0 + \sum_i \left[\frac{1}{2}\frac{\partial^2 E}{\partial D_i^2}\delta_i^2 + \frac{\partial^2 E}{\partial D_i \partial D_{i+1}}\delta_i\delta_{i+1}\right] \quad (7)$$

The mixed partial derivatives come from the nonadditivity of the interaction potential, giving rise to an additional second nearest-neighbor force constant because of the 3-atom connection. The hessian matrix is tridiagonal.

In a dimerized chain, the nearest-neighbor force constant $\frac{\partial^2 E}{\partial D_i^2}$ is either k_S or k_L, respectively, for the short and long interatomic distances. The next nearest-neighbor force constants $\frac{\partial^2 E}{\partial D_i \partial D_{i+1}} = \frac{\partial^2 E}{\partial D_S \partial D_L} = k_{nn}$ are all identical as the D_i are alternatively D_S and D_L (Figure 1).

The force on the atom number n is given by the derivative of the energy U with respect to u_n. The parameter u_n is contained in the five terms δ_{n-1}^2, δ_n^2, $\delta_{n-2}\delta_{n-1}$, $\delta_{n-1}\delta_n$, and $\delta_n\delta_{n+1}$.

We put $R = \sqrt{D_{n-1}^{-2q} + D_n^{-2q}}$ independent of n in a dimerized structure.

Standard calculations[25–27] give the equation of motion

$$(k_{n-1} + k_n - 2k_{nn})u_n - (k_{n-1} - 2k_{nn})u_{n-1} - (k_n - 2k_{nn})u_{n+1}$$
$$- k_{nn}u_{n-2} - k_{nn}u_{n+2} = -m\frac{\partial^2 u_n}{\partial t^2} \quad (8)$$

In a dimerized structure with $D_{n-1} = D_S$ and $D_n = D_L$ (Figure 1)

$$\frac{\partial^2 E}{\partial D_S^2} = q\frac{p+1}{D_S^{p+2}} - \frac{q(2q+1)}{D_S^{2q+2}}\frac{\sqrt{2}}{R} + \frac{q^2}{D_S^{4q+2}}\frac{\sqrt{2}}{R^3} = k_S$$
$$\frac{\partial^2 E}{\partial D_L^2} = q\frac{p+1}{D_L^{p+2}} - \frac{q(2q+1)}{D_L^{2q+2}}\frac{\sqrt{2}}{R} + \frac{q^2}{D_L^{4q+2}}\frac{\sqrt{2}}{R^3} = k_L \quad (9)$$
$$\frac{\partial^2 E}{\partial D_S \partial D_L} = \frac{q^2}{\sqrt{2}D_S^{2q+1}D_L^{2q+1}}\frac{1}{R^3} = k_{nn}$$

In the absence of distortion $k_S = k_L = q(p - 2q)$ and $k_{nn} = q^2$. The latter is relatively independent of the nature of the constituent atoms.[20] On the contrary, the two nearest-neighbor force constants k_S and k_L vary with the nature of the atoms, through the p parameter.

From (8) one gets the phonon dispersion relations, sum of two contributions from the nearest neighbors, unequal in the distorted structure, and the next nearest neighbors.

Let us remark that an early study[28] on the vibrational properties of (distorted) R-3m bismuth shows that the second-nearest neighbor interactions are essential to get the correct dispersion relation of Bi.

In the next two figures, the phonon dispersion relations ($0 \leq ka \leq \frac{\pi}{2}$) are shown for increasing values of the pressure that decrease the amplitude of the Peierls distortion.

3.1. Phonon Dispersion Relations

In a limited pressure range close to P_C, a dramatic change in the distribution of phonon modes occurs. The optical phonons are the most sensitive to the pressure, specially in the small k domain. We first consider the range of pressure below P_C, which corresponds to the case of PCMs. The structure is Peierls distorted, with different amplitudes as a function of the pressure. At low pressure and high distortion rate, a fairly flat band of optical frequencies appears. When the distortion (and the volume) decreases with pressure, the optical modes widen considerably in frequency and converge toward the acoustic modes (**Figure 4**).

The distortion vanishes at a transition pressure P_C (in our dimensionless units, $P_C = 0.102$) and so does the Peierls energy ΔE_P (3) as a function of η and the α parameter (Equation (4)). The electronic gap is zero (incipient metal) and the potential in η has a vanishing harmonic contribution.[13]

At P_C (**Figure 5**), the optical curve coincides with the acoustic curve because the first-neighbor force constant vanishes ($k_L = k_S = 0$). Only the second-nearest neighbor force constant is active. The two sublattices (odd and even atoms) move independently; they are decoupled at P_C. This qualifies the PCMs for thermoelectric materials.[29]

Similar results have been obtained in carbyne.[30]

In this 1D model, we only show the dispersion relations because the vibrational density of states is peculiar in 1D with divergencies at the band edges (except $k = 0$), contrary to the 3D density of states which goes smoothly to zero at the band edges as seen in the measured phonon densities of states (**Figure 6**).

The results of Figure 4 are in agreement with the experimental data obtained by inelastic neutron scattering.[14,15,31,32] With a density difference as low as 6%, the vibrational densities of states
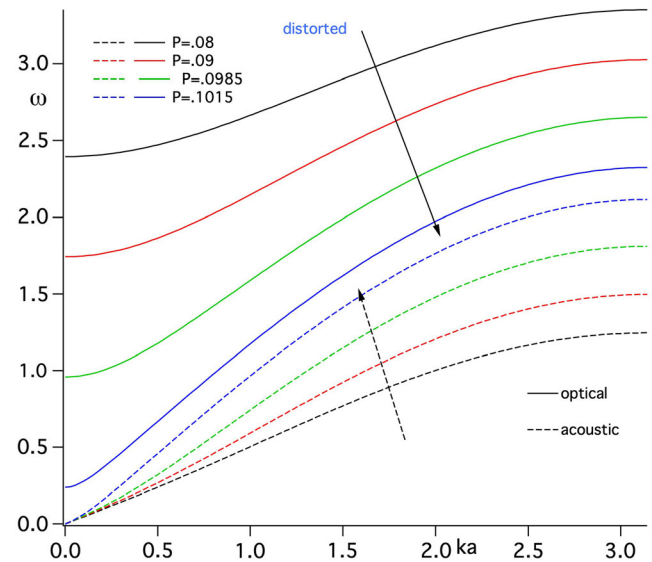

Figure 4. Evolution of the dispersion relations $\omega(ka)$ below the transition pressure P_C. The arrow indicates the pressure increase. The optical branch (full line) evolves faster than the acoustic branch (broken lines). They converge toward each other when the pressure increases.
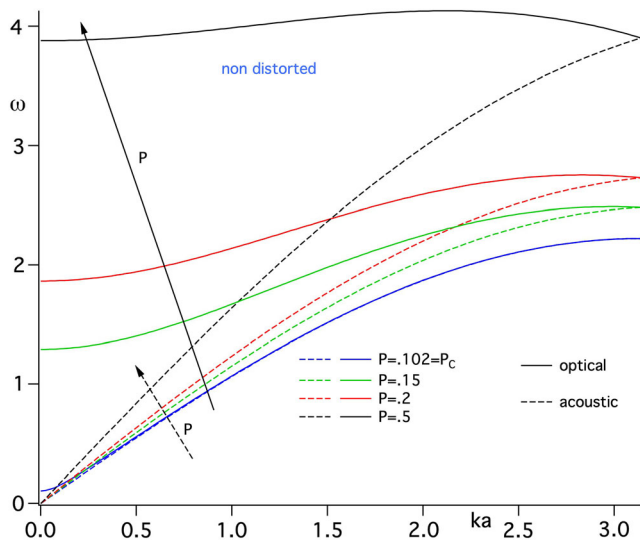
ADVANCED
SCIENCE NEWS
www.advancedsciencenews.com

physica
status
solidi **pss** **rrl**
www.pss-rapid.com

Figure 5. Evolution of the dispersion relations $\omega(ka)$ at and above the transition pressure P_C. The arrow indicates the pressure increase. The optical branch (full line) goes up with pressure faster than the acoustic branch (broken lines). For comparison with Figure 4, the lattice parameter a is unchanged although the system is now undistorted.
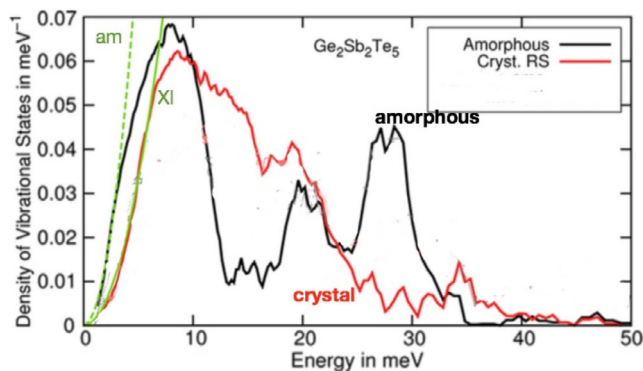
Figure 6. Densities of vibrational states of $Ge_2Sb_2Te_5$; adapted with permission.[14] Copyright 2014, American Chemical Society. In the amorphous phase, the acoustic (around 8 meV) and optical (around 28 meV) bands are well identified unlike the crystalline phase where they are merged. This corresponds, respectively, to two sections left and right of Figure 7.

of the amorphous and crystalline phases of $Ge_2Sb_2Te_5$ are very different.

In the amorphous phase, the optical and acoustic vibrations are in well-separated energy domains (Figure 6): the acoustic band is in the range [0, 12] meV with a maximum around 8 meV while the optical band has its maximum around 28 meV, well identified, unlike the crystalline phase, weakly Peierls distorted, for which both bands are totally merged, in agreement with **Figure 7** (crystal). At P_C and above, the system is no longer Peierls distorted (Figure 5); the atoms are equally spaced; however, the phonon dispersion relations are very different from the textbook case where the optical curve is above the acoustic curve. The anomalous behavior of the optical dispersion relations is related to the anharmonicity of the potential. Just above P_C the dispersion relation has still some reminiscence
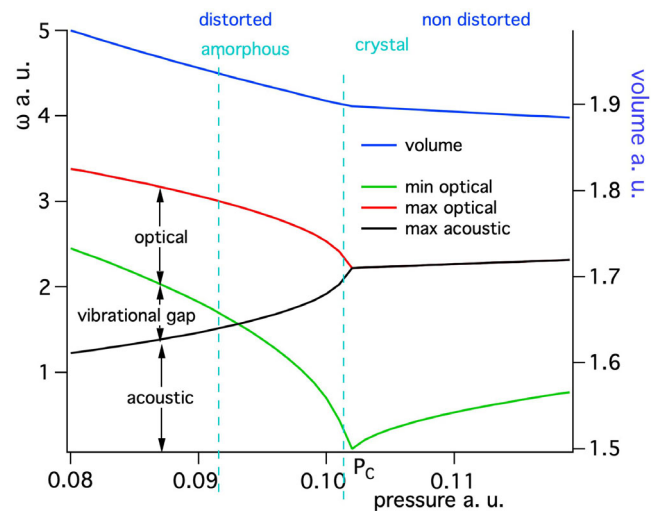
Figure 7. Frequency extrema (left scale) of the acoustic and optical modes of vibration as a function of the pressure. A vibrational gap—if any—occurs between the top of the acoustic band (black curve) and the bottom of the optical band (green curve). The vibrational gap closes before the closure of the electronic gap (incipient metal) at P_C. The light blue broken lines suggest the position of the amorphous and crystalline phases of a typical PCM with a linear difference of 2% between the two phases (6% in 3D). The volume (upper blue curve, right scale) has a larger slope in the distorted structure than in the nondistorted structure.

of the Peierls distorted case even if the distortion is no longer present. At higher pressures, a gradual evolution is observed: the optical dispersion relations go up anew with pressure as shown in Figure 5.

Figure 7 summarizes the evolution of the phonon band extension (support of the dispersion relations) as a function of the pressure. At low pressure (large distortion), the two bands, acoustic and optical, are nonoverlapping with a vibrational gap in between. The vibrational gap closes before the closure of the electronic gap (incipient metal) at P_C.

In a 1D chain, an electronic gap appears when the structure is dimerized (here below P_C) with a gap width equal to $2(\sigma(D_S) - \sigma(D_L))$. The light blue broken lines suggest the position of the amorphous (left) and crystalline (right) phases of a typical PCM with a linear difference of 2% between the two phases (corresponding to 6% in 3D). A similar behavior is found in, e.g., GeSe.[33]

The volume (upper blue curve) evolves with pressure differently in the distorted structure and in the nondistorted structure. This is obvious as in the distorted structure; the long bonds are more compressible than the short bonds.

3.2. Sound Velocity

The sound velocity v_s, slope at $k = 0$ of the acoustic dispersion relation, increases with pressure, as usual, as already observed in Figure 4.

At the equilibrium in the absence of distortion, the dispersion relation is the sum of two contributions, from the first- and second-nearest neighbors

$$m\omega^2(k) = q(p - 2q)\sin^2\left(\frac{ka}{2}\right) + q^2\sin^2\left(\frac{ka}{2}\right)$$

$$= q(p - q)\sin^2\left(\frac{ka}{2}\right) \tag{10}$$

where m is the average atomic mass of the atoms. In the limit $k \to 0$, the sound velocity is $v_s = \frac{a}{2\sqrt{m}}\sqrt{q(p-q)}$. It increases with the hardness p of the potential. The increase of v_s is very fast just below P_C (**Figure 8**), i.e., in the region corresponding to crystallization. The crystalline metallic structure, less distorted than the amorphous structure, has a higher sound velocity, and then slowly increasing above P_C. The crystallization hardens the structure.[12]

In conclusion, the covalent model (6) resolves the apparent contradiction that, upon crystallization, the acoustic modes harden while the optical modes soften.[25] The softening of the optical modes is merely a widening of the optical dispersion curves to the low frequencies. These peculiar vibrational properties induce peculiar thermomechanical properties (Grüneisen parameter and negative thermal expansion (NTE)).

4. Grüneisen Parameter

The Grüneisen parameter γ is one of the most characteristic parameters of the PCMs as it varies dramatically around the semiconductor–metal transition,[5,13] unlike conventional semiconductors or metals. This spectacular behavior is due to the Peierls distortion.

The coefficient of thermal expansion is $\beta = \frac{1}{V}\frac{\partial V}{\partial T} = \chi_T \frac{C_v}{V}\gamma$ where χ_T is the isothermal compressibility, C_v the heat capacity at constant volume, and γ the dimensionless Grüneisen parameter. The sign of the Grüneisen parameter determines whether the thermal expansion is positive or negative.

There are many definitions of the Grüneisen parameters.[34] We choose the mode Grüneisen parameter

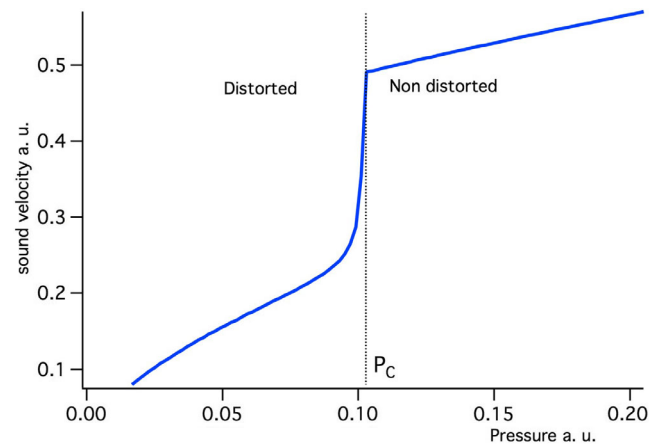$$\gamma_{k,i} = -\frac{V}{\omega_{k,i}}\frac{\partial \omega_{k,i}}{\partial V} \tag{11}$$

where i stands for the band (acoustic or optical), and k is the reciprocal coordinate. The mean Grüneisen parameter is defined by

$$\gamma = \sum_{k,i}\gamma_{k,i}C_{k,i}/C_v \tag{12}$$

where $C_{k,i}$ is the specific heat per mode. The Grüneisen parameters are weakly dependent on the temperature and we will neglect their thermal variation.

Figure 9 shows the origin of the special behavior of the Grüneisen parameters in systems that undergo a Peierls transition. The blue curve is the average Grüneisen parameter. It shows a divergence around a dimensionless transition pressure of 0.102 that corresponds to a p/q ratio of 1.8 typical of the Ge$_2$Sb$_2$Te$_5$ compound. Unfortunately, many publications mention the absolute value of the Grüneisen parameter; its sign is also interesting.

Above the transition pressure P_C, i.e., for small volumes, the frequencies of all vibrational modes increase with pressure (decrease with the volume) (Figure 5) and the Grüneisen parameters γ_i are positive; hence, the thermal expansion is positive (PTE), the normal way.

At the transition pressure P_C, the Grüneisen parameter diverges and changes sign (Figure 9). The low energy part of the optical dispersion relation contributes the most on this effect (green curve). The acoustic dispersion curve on the contrary has a quite a normal behavior.

Below the transition pressure P_C, the frequencies of the acoustic modes increase with pressure (Figure 7) giving a positive partial contribution to the Grüneisen parameter γ. At the opposite, the optical modes decrease with pressure contributing negatively to the Grüneisen parameter. In the balance between these two competing effects, the lowest optical modes, strongly pressure dependent (green curve of Figure 7), play the dominant role in the NTE.

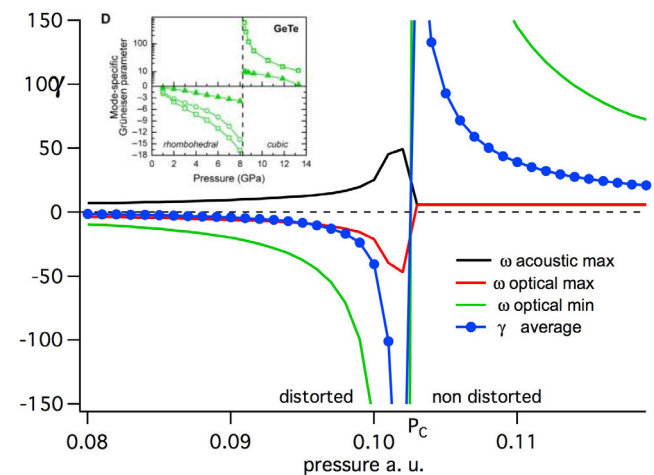At still lower pressures, possibly negative, the positivity of γ is restored.

Figure 8. The sound velocity is increasing at any pressure with a sharp increase just below P_C.

Figure 9. Average Grüneisen parameter γ (blue curve) and its components as a function of the pressure. The dominant effect comes from the lower branches of the optical phonons (in green). Inset: transverse optical phonons of GeTe; adapted with permission.[5] Copyright 2018, Wiley-VCH.
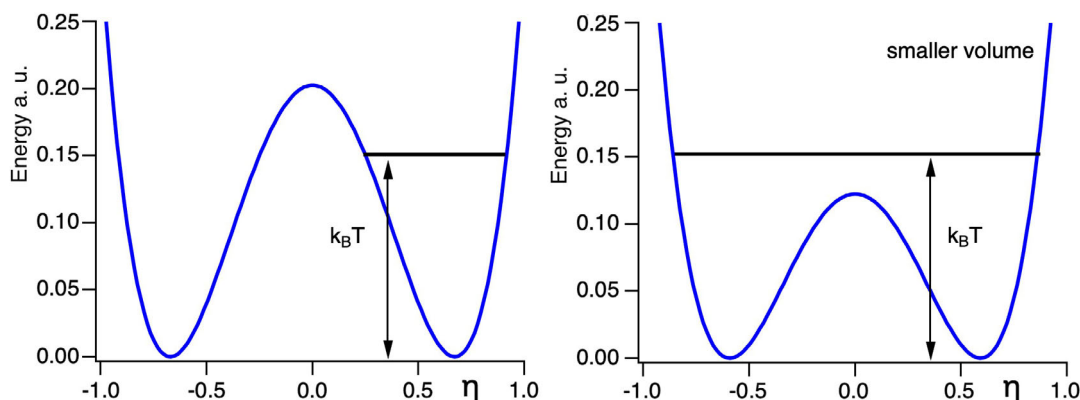
Figure 10. The volume decreases from left to right. Consequently the barrier between the two wells diminishes. The vibration at the same energy k_BT has a larger amplitude and a larger entropy in the right panel.

In conclusion, the lower branches of the optical modes play the major role.

5. Vibrational Entropy and NTE

NTE is the exception in covalent materials. It occurs mainly in Te compounds, at composition reminiscent of those of PCMs, in the liquid state, just above the melting temperature.[15,16] The origin of NTE can be explained by simple handwaving arguments.

The structure is the result of the balance between the cohesive energy and the entropy and consequently its volume. When temperature increases, the entropy starts playing an important role. In a Peierls distorted structure, the atoms vibrate in a shallow potential well (**Figure 10** left). Should the volume decrease, the system gets closer to a vanishing harmonicity with an increase of the vibrational entropy. Indeed, the vibration amplitude gets larger/wider (Figure 10 right). The thermal expansion is always in the direction of increasing entropy. Here, the entropy increases when the volume shrinks because the system is Peierls distorted. In model (6), the vibration occurs around a temperature, given by the Peierls, $T_t = \frac{\Delta E_P}{k_B}$. One can demonstrate that the entropy is maximum at the vanishing harmonicity conditions (=incipient metal).

An alternative view is the following. If the frequency of a vibrational mode ω_i decreases (resp. increases) with the volume, its contribution to the partial entropy S_i increases (resp. decreases) and the corresponding Grüneisen parameter γ_i is positive (resp. negative). The acoustic mode frequencies decrease with volume giving a positive partial Grüneisen parameter γ_i and contributing to a positive thermal expansion. At the opposite, the optical modes increase with volume ($P < P_C$) giving a negative partial Grüneisen parameter γ_i. As the lower modes of the optical modes are severely volume dependent (green curve of Figure 7), they play the dominant role in the NTE. This explains that systems close to the vanishing Peierls distortion show a NTE.

6. Conclusion

A simple model of the covalent bonding may account for the characteristic properties of PCM. In particular, it shows, qualitatively, the original trends of the vibrational spectrum. It allows explaining the apparently counterintuitive behavior: hardening of the elastic properties and softening of the optical phonons upon crystallization. In addition, it shows why PCM are good candidates for themoelectric materials and it shed some light on the NTE mechanism of compounds that undergo a Peierls transition. It originates from the singular behavior of the Grüneisen parameter. The Grüneisen parameter diverges and changes sign at the transition, when the harmonic contribution vanishes.

Conflict of Interest

The author declare no conflict of interest.

Data Availability Statement

The data that support the findings of this study are available from the corresponding author upon reasonable request.

Keywords

[1] S. R. Ovshinsky, *Phys. Rev. Lett.* **1968**, *21*, 1450.
[2] M. Wuttig, N. Yamada, *Nat. Mater.* **2007**, *6*, 824
[3] R. Jones, *J. Phys.: Condens. Matter* **2018**, *30*, 153001.
[4] K. Shportko, S. Kremers, M. Woda, D. Lencer, J. Robertson, M. Wuttig, *Nat. Mater.* **2008**, *7*, 653.
[5] M. Wuttig, V. L. Deringer, X. Gonze, C. Bichara, J.-Y. Raty, *Adv. Mater.* **2018**, *30*, 1803777.
[6] T. H. Lee, S. R. Elliott, *Phys. Status Solidi RRL* **2021**, *15*, 2000516.
[7] a) R. Peierls, *Quantum Theory of Solids*, Oxford Un. Press **2001**; b) *Les Houches lecture notes* (unpublished, 1953).
[8] J.-P. Gaspard, F. Marinelli, A. Pellegatti, C. Bichara, *Philos. Mag.* **1998**, *119*, 727.
[9] J.-Y. Raty, M. Wuttig, *J. Phys. D: Appl. Phys.* **2020**, *53*, 234002.

[10] U. Argaman, D. Kartoon, G. Makov, *J. Phys.: Condens. Matter* **2019**, *31*, 465501.

[11] D. Kartoon, U. Argaman, G. Makov, *Phys. Rev. B* **2018**, *98*, 165429.

[12] T. Matsunaga, N. Yamada, R. Kojima, S. Shamoto, M. Sato, H. Tanida, T. Uruga, S. Kohara, M. Takata, P. Zalden, G. Bruns, I. Sergueev, H. Christian Wille, R. Pierre Hermann, M. Wuttig, *Adv. Funct. Mater.* **2011**, *21*, 2232 .

[13] J.-P. Gaspard, *Phys. Status Solidi RRL* **2021**, *15*, 2000536.

[14] P. Zalden, K. S. Siegert, S. Rols, H. E. Fischer, F. Schlich, T. Hu, M. Wuttig, *Chem. Mater.* **2014**, *26*, 2307.

[15] C. Otjacques, J. Y. Raty, M. V. Coulet, M. Johnson, H. Schober, C. Bichara, J. P. Gaspard, *Phys. Rev. Lett.* **2009**, *103*, 245901.

[16] C. Otjacques, J. Y. Raty, F. Hippert, H. Schober, M. Johnson, R. Céolin, J. P. Gaspard, *Phys. Rev. B* **2010**, *82*, 054202.

[17] F. Cyrot-Lackmann, *Adv. Phys.* **1967**, *16*, 393.

[18] a) R. Hoffmann, *Angew. Chem., Int. Ed.* **1987**, *26*, 846; b) R. Hoffmann, *Solids and Surfaces. A Chemist's View of Bonding in Extended Structures*, VCH, New York **1988**.

[19] J.-P. Gaspard, *C. R. Phys.* **2016**, *17*, 38905.

[20] W. A. Harrison, in *Electronic Structure and the Properties of Solids* (Ed. W.H. Freeman), W.H. Freeman &Co, San FranciscoNew-York **1980**.

[21] G. Mie, *Ann. Phys.* **1903**, *316*, 65797.

[22] F. Ducastelle, *J. Phys.* **1970**, *31*, 1055.

[23] D. Pettifor, *Bonding and Structure of Molecules and Solids*, Clarendon Press, Oxford **1995**.

[24] W. K. Njoroge, H.-W. Woltgens, M. Wuttig, *J. Vac. Sci. Technol., A* **2000**, *20*, 23033.

[25] M. Dove, *Introduction to Lattice Dynamics*, Cambrige University Press, Cambridge **1993**.

[26] N. Ashcroft, D. Mermin, *Solid State Physics*, Harcourt Brace&Co, Fort Worth **1976**.

[27] H. Schober, S. Rols, *Collect. SFN* **2010**, *10*, 336.

[28] J. L. Yarnell, J. L. Warren, R. G. Wenzel, S. H. Koenig, *IBM J. Res. Dev.* **1964**, *8*, 3.

[29] Y. Yu, M. Cagnoni, O. Cojocaru-Mirdin, M. Wuttig, *Adv. Funct. Mater.* **2019**, *30*, 1904862.

[30] A. Milania, M. Tommasini, G. Zerbi, *J. Chem. Phys.* **2008**, *128*, 064501.

[31] P. Zalden, F. Quirin, M. Schumacher, J. Siegel, S. Wei, A. Koc, M. Nicoul, M. Trigo, P. Andreasson, H. Enquist, M. J. Shu, T. Pardini, M. Chollet, D. Zhu, H. Lemke, I. Ronneberger, J. Larsson, A. M. Lindenberg, H. E. Fischer, S. Hau-Riege, D. A. Reis, R. Mazzarello, M. Wuttig, K. Sokolowski-Tinten, *Science* **2019**, *364*, 1062.

[32] U. D. Wdowik, K. Parlinski, S. Rols, T. Chatterji, *Phys. Rev. B* **2014**, *89*, 224306.

[33] V. L. Deringer, R. P. Stoffel, R. Dronskowski, *Phys. Rev.B* **2014**, *89*, 094303.

[34] J. P. Poirier, *Introduction to the Physics of the Earth's Interior*, Cambridge University Press, Cambridge **1991**.